

Pricing Spot Electricity Options
under a
Mean Reverting Jump Diffusion Model

Sz.B. Gaál

Contents

1	Introduction	3
1.1	Deregulation of electricity markets	3
1.2	Spot electricity prices	4
1.3	Characteristics of electricity	5
2	Overview of models for electricity prices	8
2.1	Diffusion models	8
2.2	Jump diffusion models	9
2.3	Regime switching	10
2.4	Other models	10
2.5	Choosing a model	11
2.6	Stochastic calculus: a digression	11
3	A jump diffusion model	14
3.1	Specification of the spot electricity model	14
3.2	Option pricing on spot electricity	15
3.3	Convenience yield	16
3.4	Risk free versus risk based pricing	16
4	Numerical methods	19
4.1	Fourier expansion	19
4.2	Finite Difference - Finite Elements	22
4.3	Numerical results	26
5	Parameter estimation	33
5.1	Different estimation methods	33
5.2	Theoretical conditional characteristic function	33
5.3	Empirical characteristic function	35
6	Conclusion	39
A	Inner product convolution and test function	40
B	Essent	42
C	References	43

Abstract

The goal of this report is twofold. Firstly, we introduce in chapter 1 the reader to electricity markets and the Dutch APX in particular. After that in chapter 2 we discuss available models for the spot electricity price in the literature. Secondly, we introduce a model which captures both spikes and mean-reversion, and price an European put option under this model.

We model in chapter 3 the spot electricity market as a double exponential jump diffusion process, originally due to Kou & Wang in [Kou01]. In this report we extend their work by making the process mean-reverting. To price the option we derive a backward parabolic partial integro-differential equation. In chapter 4 we give two numerical methods to solve this equation: a Fourier expansion method and a combination of the Finite Difference and Finite Elements method. The parameters of our model are estimated in chapter 5 on daily average APX-prices by means of matching the empirical to the theoretical conditional characteristic function. We conclude in chapter 6 with an overview of the results.

1 Introduction

In this section we will give an introduction to electricity markets and their spot prices. We start with the deregulation of electricity markets with particular emphasis on the Dutch situation. After that we discuss how spot electricity prices are set in the Netherlands and how energy modelling differs from traditional financial modelling. Examples of Dutch spot electricity prices are given in the last paragraph where we also discuss the characteristics of spot electricity prices.

1.1 Deregulation of electricity markets

Electricity markets all over the world are starting to become deregulated. The earliest countries to deregulate their electricity markets were Chile (1982) and New Zealand (1987), closely followed by the United Kingdom (1990), Norway (1991) and Argentina (1991).

In EU directive 96/92, see [EP97], the European Union set out the requirement to open up the electricity supply markets. It stated that the market should be open in 1999 for customers with an annual requirement of 40 GWh per year. This was to be reduced to 20 GWh per year in 2000 and 9 GWh in 2003. To speed this up, there is an EU-proposal, see [EP01], that the electricity supply market should be open totally by January 2005.

However, deregulation is done in many different ways. Around the world there are different market and ownership structures. In general governments do deregulate the generation of power, while major parts of the transmission and distribution of energy remain regulated. The Dutch transmission and major parts of the national grid is managed by TenneT, a state owned company. Essent and Nuon are examples of companies which own small parts of the grid. Essent is in a unique position in the Netherlands as it is a vertically integrated firm combining generation, transmission, trading and retail.

The idea of complete privatization of the distribution network has unsuccessfully been tested in the United States. Recent failures have caused the system to collapse and the United States is returning to a regulated distribution network.

Deregulation in the Dutch energy market is done in three phases. In the first phase in 1999 big (phase 1) customers got the freedom to choose in purchasing electricity. The second phase in 2002 made it possible for medium customers to choose whereas the households get this freedom only if they choose for green energy. The final phase in 2004 will lead to freedom for all the customers.

The basic goal of deregulation in the Netherlands was cost reduction for the end user. It was believed that the generation of electricity would become more efficient and thus a cost reduction would be achieved compared to the completely regulated market. Some result of deregulation in the Netherlands will become clear from figure 2.

Due to deregulation, trading of electricity has become common practice as has always been the case for trading of commodities. For commodities a lot of

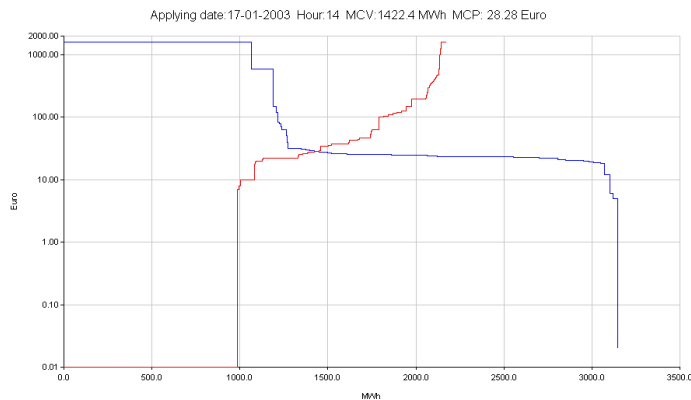


Figure 1: APX supply stack for 17-01-2003, hour 14. Note prices are in a log scale

literature has been developed, which however cannot be applied directly to the electricity market. This is explained subsequently.

1.2 Spot electricity prices

In the Netherlands short term trading is done at the Amsterdam Power Exchange (or APX) which is a day ahead forward market. We will denote the APX price by the spot price. The Dutch spot electricity price is set by TenneT after bids from all generators. TenneT collects prices and volumes from generators and matches it to the actual demand for every hour of the day. In this way a supply stack appears as in figure 1. The supply graph is sloping upwards, while the demand graph is sloping downwards. The intersection of the two graphs gives the spot price, which in this case is 28.28 Euro per MWh.

On the supply side we can classify the generating units in base load, mid merit and peak load by the costs of running. Base load units usually run 24 hours a day, while peak-load only run if other units fail.

On the demand side most interesting is the long horizontal part in the middle of the graph. It means demand can grow from 1200 to 3200 MWh in case of relative small price changes. It can be explained by the specifics of the Dutch generation park. If the spot price is low enough (that is: under the cost price of a plant plus compensation for shut down and startup), the producer rather shuts down his plant than risking a failure. In the Netherlands we indeed have several gas plants with these features.

Besides this price dependence demand is driven by the heating and cooling needs of consumers. So, besides seasonal (predictable) changes in the weather,

unpredictable day to day weather changes play a major role in the electricity price.

Looking around the world we observe different market and ownership structures as well as different weather conditions and generation parks. Still there are striking similarities between the electricity prices. Del Buono offers in [DelB00] a comparison between electricity markets in Spain, Australia, Norway, Canada (Alberta) and the United States (California). He argues there characteristics of electricity prices are due in most part to the physical characteristics of electricity rather than market design.¹

The main difference between commodities and electricity is the non-storability of electricity: it is hard and expensive to store on a low scale and as far as we know impossible on industry scale (disregarding the limited storage one can achieve with hydro plants, which are not available in the Netherlands.) Moreover, to keep the network functioning there is a need for balance between supply and demand which, in combination with the lack of inventories, leads to volatile spot prices and quick jumps in the spot price. If we combine this fact with the seasonal patterns of electricity prices, it is intuitive that modelling the electricity market is complicated. Moreover, option pricing will encounter problems as most arbitrage arguments are based on storage. This will become particularly clear in section 3 where we discuss our spot electricity model.

The introduction of the spot market meant a creation of an underlying for power derivative contracts. In the Netherlands most contracts are forwards, which are traded OTC. Besides forwards, a variety of European and Asian options are traded. In these contracts we distinguish between a whole day delivery (or base load), special business hours (07 to 23 or peak load) and specific hours. Specific hours are traded only a few days in advance, while base load and peak load are traded a few years out.

1.3 Characteristics of electricity

Within the electricity market we observe a mean-reversion effect in the spot prices towards a level slightly above production costs. This effect can, for long lasting events, be attributed to changes in supply due to a high price (increase production) or low price (decrease production). Short lasting events can simply stop (e.g. a plant starts working again) and a return to the standard level is achieved.

Besides this mean-reversion effect there are factors as weather and production failures of a producer, which have a short lasting but major impact on the price level. For this reason we observe within the electricity market large jumps in the spot price.

The Dutch electricity market is known for frequent and high spikes in comparison to most other electricity markets. To show the order of price movements we present here a few representative graphs from the APX.²

¹Del Buono offers a supply stack for Spain where demand does not show a horizontal line like in the Dutch situation. This can be attributed to the design of the Spanish market.

²APX provides all data freely on their website: www.apx.nl

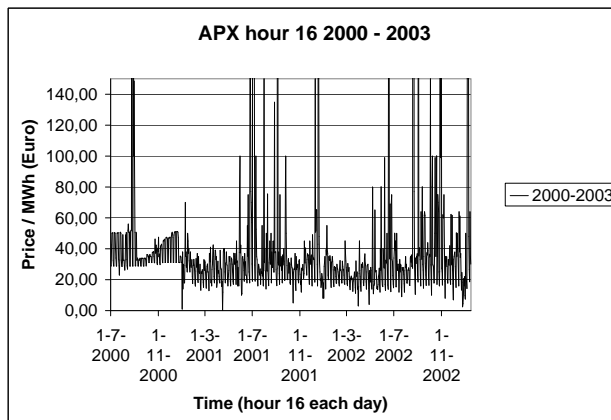


Figure 2: APX hour 16. Note prices are truncated at 150 Euro

In figure 2 we show a result of deregulation. From 1-7-2000 until 1-1-2001 the market was still more or less regulated. The date 1-1-2001 is clearly visible as the day the market started to move more intense. Since that date there is a higher variance and the price drops regularly under 30 Euro per MWh. Note that this graph is created by taking a single hour (hour 16) per day for all days.

In the same figure we can see that the market behaved quite differently in 2001 and 2002. Taking a closer look at the recent year is done in figure 3a which shows a base load picture of the year 2002 with average prices per day. A frequency plot of the same data is given in figure 3d. Immediately it is clear that the distribution is not symmetric and has a fat right tail. The prices are not moving according to a yearly pattern, possibly indicating a non-mature market.

There is a strong predictable effect in spot electricity prices through the day as we can see in figure 3c. Hourly data from the week 15-21 April 2002 shows a big peak around noon and a smaller peak around 18:00 hours. Prices are consistently lower for the night: the base load units have to run and the unsold portion of the generated electric energy must eventually be damped.

Finally we show a predictable effect in spot electricity prices through the week. In figure 3b we take a closer look at data from April 2002, where we used the average of the APX base load price per day to filter out the daily pattern. We see the price drops in the weekend with Sunday's price just a little lower than Saturday's price.

In this project we are looking for a suitable model for the spot electricity prices in the Netherlands. From the above we conclude our model should include mean-reversion and jumps.

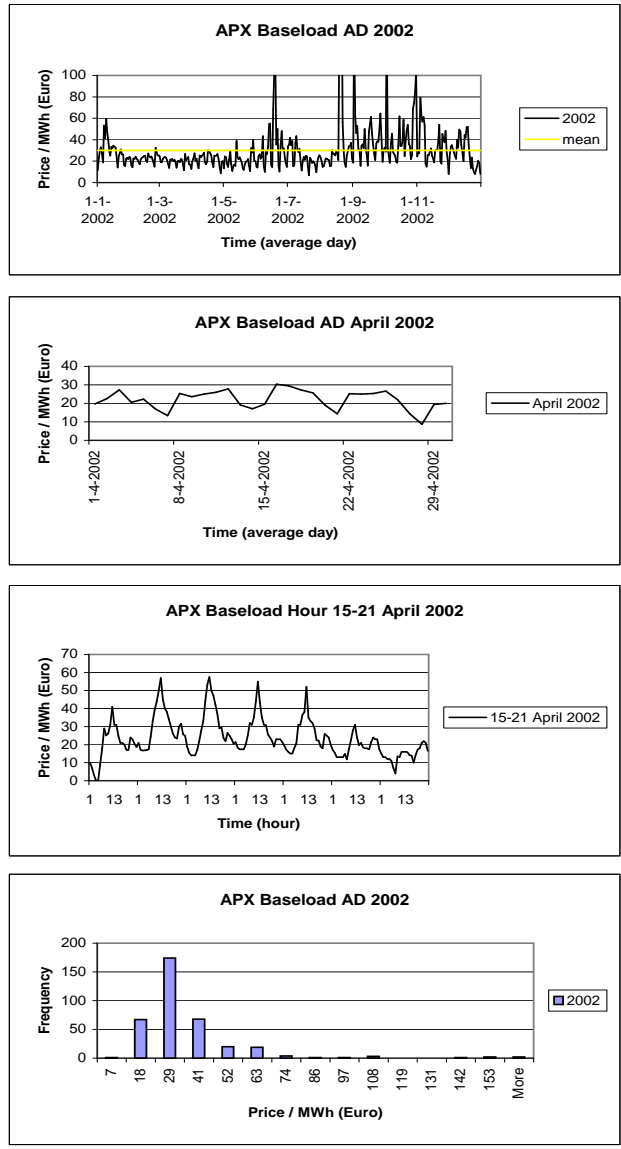


Figure 3: a) shows average APX per day base load 2002, b) shows average APX per day base load in April 2002, c) specializes to the third week in April 2002 (hourly APX price), d) gives the frequency plot of average APX prices per day base load 2002

2 Overview of models for electricity prices

Within the literature on modelling electricity prices there are two different approaches. One invokes a fundamental analysis describing market behavior via the available supply and demand. Within electricity markets supply and demand must be equal and one can find an equilibrium price. The other, which we pursue here, is based on a quantitative analysis, which describes market behavior via mathematical methods and statistical techniques.

In this section we give an overview of models which have been proposed in the literature. We start with diffusion models after which we discuss jump diffusion models in detail. In paragraph 2.3 we discuss the regime switching models and in paragraph 2.4 we mention more general models containing non-constant volatility and several underlying factors.

In paragraph 2.5 we use criteria like mean-reversion, jumps and computational ease to make a choice between all models for the spot electricity price. Our choice will be to develop a mean-reverting version of the double exponential jump diffusion model originally due to Kou & Wang in [Kou01]. To describe such a model we need the Ito calculus for compound Poisson processes, which will be discussed in the last paragraph of this section.

2.1 Diffusion models

The common starting point for modelling usual assets is the Geometric Brownian Motion (or GBM) model. It is quite reasonable for usual assets and simple enough to lead to analytical formulas. It describes the change in price dS as follows:

$$dS(t) = \mu S(t)dt + \sigma S(t)dW(t) \quad (1)$$

where μ and σ are constants denoting the drift rate and volatility, and W a standard Brownian motion. One can show that S is lognormally distributed with a variance growing linearly with time. As we observe a bounded variance of prices in the electricity market and a long term mean this model seems not appropriate for electricity. As noted in the first section, within electricity markets there is a need for mean-reversion in the prices towards some kind of equilibrium level. A natural extension of the GBM model is the geometric mean reversion model (or GMR) model.

$$dS(t) = \kappa[\alpha - \ln S(t)]S(t)dt + \sigma S(t)dW(t) \quad (2)$$

where κ the rate of mean reversion, α is the logarithm of the long term mean and σ is the volatility.

Both the GBM and GMR models are formulated in a log-normal setting, which prevents prices from becoming negative. Besides this formulation models are also formulated in a normal setting. Mean-reversion models can then be formulated as

$$dS(t) = \kappa[\bar{\alpha} - S(t)]dt + \sigma S(t)^\gamma dW(t) \quad (3)$$

where $\bar{\alpha}$ is the long term mean and γ controls the price-dependency of the volatility. For the case $\gamma = 0$ we get back to the simplest mean-reverting model known as the Ornstein-Uhlenbeck model:

$$dS(t) = \kappa[\bar{\alpha} - S(t)]dt + \sigma dW(t) \quad (4)$$

One of the problems of this model is that prices can become negative, which we do not observe in the electricity market. In the case $\gamma = 1$ prices are non-negative and we have price proportional volatility as investigated by Del Buono in [DelB00]:

$$dS(t) = \kappa[\alpha - S(t)]dt + \sigma S(t)dW(t) \quad (5)$$

Del Buono found this model to be superior to the models in (1), (2) and (4) by comparing their distributions with empirical ones in the United States (California), Spain, Australia, Canada (Alberta) and Norway.

Another special case known from the modelling of the term structure of interest rates is the case $\gamma = \frac{1}{2}$. It is better known as the Cox-Ingersoll-Ross (or CIR) model:

$$dS(t) = \kappa[\alpha - S(t)]dt + \sigma\sqrt{S(t)}dW_t \quad (6)$$

2.2 Jump diffusion models

An extension of the above class of models is the one that introduces jumps into the price process. These models reflect the fact that we do see discontinuities in the price process coming from e.g. an unplanned outage. Intuitively one would say discontinuities will become more important for short term behavior as price changes play a larger role then. This also comes out in a comparison by Barz in [Barz99] who showed that adding jumps to the GMR model (compared to GBM, GMR and GBM with jumps) is most appropriate for modelling short term electricity price changes via a log-likelihood comparison and economical justification. However, he notes that GMR without jumps better characterizes the long term distribution of prices near their mean than GMR with jumps. This can be attributed to the following: including jumps gives a better fit to extreme events of low probability, which leads to a decrease in κ .

To extend the class of diffusion models the common choice is a compound Poisson process. In general one can say the Brownian motion takes care of a continuous noise, while the compound Poisson process takes care of discontinuities. A mixture of a compound Poisson process and a Brownian motion can thus provide us a process containing both random noise and jumps.

Jumps are often modelled by a compound Poisson process where the size and timing of the jumps are independent. The first jump diffusion model is from Merton in [Mert76] who draws the jump size from a normal distribution.

Kou and Wang work in [Kou01] on another jump diffusion model where the jump size is drawn from a double exponential distribution. This model can explain asymmetric return distributions which are skewed to the right, and the volatility smile. These are two characteristics of spot electricity prices observed in the market.

Jump diffusion models have also been applied to model forward curves (see e.g. [Glas03]) and bond markets (see e.g. [Bjor97]).

2.3 Regime switching

A model quite similar to jump diffusion is the model of regime switching. According to this model there are different states a process can be in. The two-state regime switching model classifies the process in an ‘abnormal’ (high price) and ‘normal’ (low price) state with a possible transition between them. In other words: it is a model which identifies switching regimes. Three references on these models are [Hami90], [Deng99] and [Khol01].

The link with jump diffusion models becomes clear if we let the regime switching have small duration in a high state which then can be compared to a jump. Other extensions the regime switching model can bring are the following. Firstly regime switching can allow to have two totally different underlying processes in the two states. This corresponds to unnatural behavior in a high state. Regime switching can also capture the distinction between different plants as in peak load, mid-merit and base load by introducing three different regimes.

2.4 Other models

Besides the diffusion, jump diffusion models and the regime switching mentioned above, there are several other models available in the literature. In all the above models volatility is assumed to be constant. Relaxing this assumption gives rise to time and price dependent volatility.

Modelling of the evolution of the locally deterministic volatility surface in a continuous setting is done by Dupire in [Dupi94]. More popular however is the stochastic volatility model as proposed by Heston in [Hest93]. His model (containing two different standard Brownian motions which are correlated) is the following:

$$\begin{aligned} dS(t) &= \mu S(t)dt + \sqrt{v(t)}S(t)dW^1(t) \\ dv(t) &= \kappa[\theta - v(t)]dt + \sigma\sqrt{v(t)}dW^2(t) \end{aligned}$$

An extension of this is the stochastic volatility model with time changes given by Carr, Geman, Madan and Yor in [Carr03].

A generalization of the locally deterministic and stochastic volatility models is the affine jump diffusion model. In that model drift, covariance matrix and jump intensity are supposed to be affine. In general A is affine with respect to X if $A = c_1(t) + c_2(t)X$ for some constant $c_1(t)$ and $c_2(t)$. An important work regarding affine jump diffusion is [Duff00] by Duffie, Pan & Singleton. The affine

jump diffusion also allows for multi-factor models. Deng for example describes in [Deng99] models with stochastic volatility with two different underlying factors and two kinds of jumps.

Another known two-factor model is from Pilipovic in [Pilo98], who allows the long term mean to change over time. Thus the short term and long term behavior are different. A major drawback of this model is the need for very long time series to estimate the long term parameters. This kind of models might be more appropriate as a forward model than as a spot model.

Finally we want to name some advanced models from asset price modelling. Currently these are hardly applied in electricity modelling, but it might pay off to take a closer look at them. We name Variance Gamma, Normal Inverse Gaussian, Generalized Hyperbolic and Finite Moment Logstable. We will not go further into these (so called Lévy process) models and refer the interested reader to [Lew01].

2.5 Choosing a model

In this report we are looking for a mean reverting spot electricity model which captures spikes correctly. From the mentioned models we believe there are three models which show spiky behavior: price dependent volatility, jump diffusion models and regime switching.

The price dependent volatility gives spikes, but does not have the discontinuities as we do observe in the spot price. Both jump diffusion model and regime switching do exhibit this feature. Considering the time for this project, we made the choice to focus the research on jump diffusion.

We assume in our modelling the volatility σ to be constant. This assumption simplifies the calculations considerably. Moreover, with the jumps we introduce an extra source of uncertainty leading to a decrease of σ as the total uncertainty is split between the Brownian motion and the jumps.

Within the jump diffusion models we have chosen the double exponential jump diffusion model originally due to Kou & Wang mainly for its computational ease. Kou & Wang showed in [Kou01], that their model can give closed form solutions for path dependent options like barrier options and lookback options. This type of results is hard to derive for other models. That they can be obtained for the double exponential model is mainly due to the fact that exponential distributions are memoryless. Using two exponentials makes it possible to create asymmetric distributions as we saw in figure 3d.

We like to note here that the process Kou & Wang worked on is not mean-reverting, while this is a necessary feature of spot electricity prices. We have thus decided to include mean reversion in their setting.

2.6 Stochastic calculus: a digression

In the next chapter we will describe our model using ideas from stochastic calculus. In this paragraph we show how to extend stochastic calculus for Brownian motion to compound Poisson processes. We refer the reader unfamiliar with

stochastic calculus to Etheridge, [Ethe02]. Here we provide a workable version of the Ito formula for compound Poisson processes. This Ito formula is a special form of the generalized Ito formula.

Theorem 1 (Ito formula for compound Poisson processes) *Suppose $X(t)$ satisfies the stochastic differential equation*

$$dX(t) = \mu(X(t), t)dt + \sigma(X(t), t)dW(t) + dN(t) \quad (7)$$

where $\mu(\cdot, \cdot)$ and $\sigma(\cdot, \cdot)$ are adapted processes to the filtration F_t , $W(t)$ is a standard Brownian motion, $N(t)$ is a non-compensated compound Poisson process with arrival rate λ and the jump size is drawn from a distribution having a density of $g(\cdot)$.

If $f(X(t), t)$ is a continuous function of which $\frac{\partial f}{\partial t}$, $\frac{\partial f}{\partial x}$ and $\frac{\partial^2 f}{\partial x^2}$ do exist then $f(X(t), t)$ satisfies

$$df(X(t), t) = df_c(X(t), t) + df_j(X(t), t) \quad (8)$$

where

$$df_c(X(t), t) = \left[\frac{\partial f}{\partial t} + \mu \frac{\partial f}{\partial x} + \frac{1}{2} \sigma^2 \frac{\partial^2 f}{\partial x^2} \right] dt + \sigma \frac{\partial f}{\partial x} dW(t) \quad (9)$$

$$df_j(X(t), t) = \left[\int_{-\infty}^{\infty} f(x)g(y)dy - f(x_-) \right] dN(t) \quad (10)$$

where in (10) $f(x)$ denotes the function value after the jump and $f(x_-)$ the function value before the jump.

A full proof of the generalized theorem can be found in Ikeda & Watanabe, [Ikeda81]. A less technical approach to the above theorem can be found in Etheridge, [Ethe02], who gives the Ito-formula for Poisson processes with a heuristic proof.

Example: Doléans-Dade exponential formula

Here we give an example of the use of the Ito formula and see how to check that a process is a martingale. The example is partially taken from [Ethe02].

Suppose $Z(t)$ satisfies the stochastic differential equation

$$dZ(t) = \lambda(1 - e^\nu)dt + dN(t)$$

where $N(t)$ is a non-compensated compound Poisson process with arrival rate λ and fixed jump size ν . We define $L(Z(t), t) \equiv e^{Z(t)}$ and will show that it is a martingale.

According to the Ito formula in (8) the function $L(Z(t), t)$ satisfies

$$dL(Z(t), t) = dL_c(Z(t), t) + dL_j(Z(t), t)$$

To find the differential for the first part we set $\mu = \lambda(1 - e^\nu)$ and $\sigma = 0$ in (9) leading to

$$dL_c(Z(t), t) = \lambda(1 - e^\nu)L(Z(t), t)dt$$

If a jump occurs, the process jumps from $Z(t)$ to $Z(t) + \nu$. The density $g(\cdot)$ is in this case a Dirac-delta function $\delta(y - \nu)$ and the differential in (10) becomes

$$dL_j(Z(t), t) = [L(Z(t) + \nu, t) - L(Z(t), t)] dN(t)$$

Now observe

$$L(Z(t) + \nu, t) = e^{Z(t)+\nu} = e^\nu L(Z(t), t)$$

to find

$$\begin{aligned} dL(Z(t), t) &= L(Z(t), t)(1 - e^\nu) [\lambda dt - dN(t)] \\ &= L(Z(t), t)(e^\nu - 1)dM(t) \end{aligned} \tag{11}$$

where we have introduced $dM(t) = dN(t) - \lambda dt$. It can be shown this compensated Poisson process $M(t)$ is a martingale, which implies $L(Z(t), t)$ is also a martingale.

The process $L(Z(t), t)$ we have discussed here is an example of a Doléans-Dade exponential.

3 A jump diffusion model

In this section we specify our spot electricity model. The model is based on specifying the jump density in an affine jump diffusion model to be double exponential. This kind of model has been proposed before by Kou & Wang in [Kou01]. We include here a mean-reversion term and derive a parabolic partial integro-differential equation and an appropriate initial condition for the option price. In paragraph 3.3 we explain our underlying assumption for option pricing. Finally, in paragraph 3.4 we discuss how to resolve the risk inherent in jump diffusion models.

3.1 Specification of the spot electricity model

Within jump diffusion models one assumes that jumps arrive according to a Poisson process where jump sizes are taken from an unknown distribution. In [Mert76] the jumps are drawn from a normal distribution. We will assume here like [Kou01] that jumps are drawn from a double exponential distribution and that if a jump occurs the spot electricity price, denoted by S_t , changes from S_t to $S_t Y$.

Let us first recall the probabilities that a Poisson event will occur in an arbitrary small time interval of length Δt . If events arrive according to a Poisson process with mean arrival rate λ , the probability of exactly one jump event is $\lambda \Delta t + o(\Delta t)$.³ The probability that no jump event will occur is $1 - \lambda \Delta t + o(\Delta t)$, while the probability that more than one jump event will occur is $o(\Delta t)$.

Let us start by specifying our spot electricity model by giving the stochastic differential equation (or SDE)

$$\frac{dS_t}{S_t} = \kappa(\alpha - \ln S_t)dt + \sigma dW_t + d \sum_{i=1}^{N_t} (V_i - 1) \quad (12)$$

where κ , α and σ are assumed to be constant, N_t is a Poisson process with intensity λ and $\{V_i\}$ is a sequence of independent identically distributed non-negative random variables such that $Y \equiv \log V$ has an asymmetric double exponential distribution with density

$$f_Y(y) = p\eta_1 e^{-\eta_1 y} 1_{\{y \geq 0\}} + q\eta_2 e^{\eta_2 y} 1_{\{y \leq 0\}} \quad (13)$$

Imposing the restrictions $\eta_1 > 1$ and $\eta_2 > 0$ ensure the process to have finite expectation, see (17). Assuming $p > 0$ and $q > 0$ makes it possible to interpret parameters p and q as the probability of an upward, respectively downward, jump in the price. The total probability mass does equal 1

$$\int_{-\infty}^{\infty} f_Y(y) dy = p \int_0^{\infty} \eta_1 e^{-\eta_1 y} dy + q \int_{-\infty}^0 \eta_2 e^{\eta_2 y} dy \equiv 1$$

implying that parameters p and q add to 1.

³Here $o(f)$ implies $\lim_{\Delta t \rightarrow 0} \frac{f(\Delta t)}{\Delta t} = 0$

Furthermore we assume all sources of randomness, W_t , N_t and Y_i are independent. Thus the size and time of a jump are assumed to be independent and we call $\sum_{i=1}^{N_t} (V_i - 1)$, or Z_t in short, a compound Poisson process.

3.2 Option pricing on spot electricity

In this report we want to price a European put option on the process S_t given in (12). With this option one is allowed to sell spot electricity for a certain strike price K at a specified moment T in the future, but does not have the obligation to sell. In the following proposition we state our approach to find the price, denoted by $\psi(X_t, t)$, of this contract. Here $X_t = \ln S_t$ denotes the logarithm of spot price S_t .

Proposition 1 *The price, denoted by $\psi(X_t, t)$, of a European put option with strike 1 and time to maturity T is the unique solution to the following equation⁴*

$$\frac{\partial \psi}{\partial t} + \kappa(\alpha^* - x) \frac{\partial \psi}{\partial x} + \frac{1}{2} \sigma^2 \frac{\partial^2 \psi}{\partial x^2} - \lambda \psi + \lambda \int_{-\infty}^{\infty} \psi(y, t) f_Y(y - x) dy = 0 \quad (14)$$

with the initial condition

$$\psi(X_t, t)|_{t=T} = \begin{cases} 1 - e^x & x \leq 0 \\ 0 & x > 0 \end{cases} \quad (15)$$

At maturity, $t = T$, the option price is $\max\{1 - S_T, 0\}$. If $S_T < 1$, one buys electricity on the spot market and sells it under the contract. In other cases one can refrain from selling. After the transformation $X_t = \ln S_t$ we have (15).

Before maturity, $t < T$, determining the value is non trivial. Let us assume the function $\psi(X_t, t)$ is twice differentiable in x and once differentiable in t , to be able to apply Ito calculus. It yields the expected change in the value of the option, denoted by $Ed\psi(X_t, t)$, is given by

$$Ed\psi(X_t, t) = \frac{\partial \psi}{\partial t} + \kappa(\alpha^* - x) \frac{\partial \psi}{\partial x} + \frac{1}{2} \sigma^2 \frac{\partial^2 \psi}{\partial x^2} + \lambda \left[\int_{-\infty}^{\infty} \psi(x + y, t) f_Y(y) dy - \psi \right]$$

where we have introduced

$$\alpha^* \equiv \alpha - \frac{\lambda \zeta}{\kappa} - \frac{\sigma^2}{2\kappa} \quad (16)$$

and $\lambda \zeta$ is the compensator with $\zeta \equiv E[V] - 1$ given by

$$\zeta = \int_{-\infty}^{\infty} e^y f_Y(y) dy - 1 = \frac{p\eta_1}{\eta_1 - 1} + \frac{q\eta_2}{\eta_2 + 1} - 1 \quad (17)$$

Note the convolution can be rewritten to get the function $\psi(y, t)$ inside the integral via

$$\int_{-\infty}^{\infty} \psi(x + y, t) f_Y(y) dy = \int_{-\infty}^{\infty} \psi(y, t) f_Y(y - x) dy$$

⁴In order to save space we sometimes drop the arguments of $\psi(X_t, t)$ and simply write ψ

To arrive at (14) we need an extra assumption, which we take to be a zero convenience yield. In the next paragraph we will discuss this assumption in relation to the Black & Scholes assumption. Our assumption implies $Ed\psi(X_t, t) = 0$ leading to (14).

If we introduce the generator L and convolution K as follows:

$$L\psi(X_t, t) = \kappa(\alpha^* - x)\frac{\partial\psi}{\partial x} + \frac{1}{2}\sigma^2\frac{\partial^2\psi}{\partial x^2} - \lambda\psi \quad (18)$$

$$K\psi(X_t, t) = \lambda \int_{-\infty}^{\infty} \psi(y, t) f_Y(y - x) dy \quad (19)$$

then (14) can be written in short as

$$(L + K)\psi(X_t, t) + \frac{\partial\psi}{\partial t} = 0 \quad (20)$$

This is a forward parabolic partial integro-differential equation (or PIDE) describing the price of an option in the special case of a double exponential jump diffusion model. One can invert time and get a backward PIDE instead of a forward PIDE by defining $\tau = T - t$. It leads to $\frac{\partial}{\partial t} = -\frac{\partial}{\partial \tau}$ and the backward PIDE is in short

$$(L + K)\psi(X_\tau, \tau) - \frac{\partial\psi}{\partial \tau} = 0 \quad (21)$$

3.3 Convenience yield

To derive a pricing equation for the European put option in Proposition 1 we have made the assumption of a zero convenience yield. This approach is fundamentally different from the Black & Scholes assumption.

Comparing our equation with the Black & Scholes pricing equation (see e.g. [Bjor98, theorem 6.7]), one can observe the term $r\psi(X_t, t)$ in their equation, which we take to be zero. In the Black-Scholes model the price is determined by an arbitrage argument between a risk free bond and a risk free portfolio containing the option and the underlying. One of the assumptions for this argument is that one can store the underlying, which in the case of electricity is impossible on industry scale.

Our approach wants to stress there is no possibility to create a risk free portfolio. With no possibility to hold this portfolio, one assigns an arbitrary convenience yield to it, which we take to be zero.

3.4 Risk free versus risk based pricing

The virtue of the Black-Scholes model is that one is able to uniquely price an option, that is the model is complete. One can transform the measure from the underlying objective probability measure (which is used to observe the price of the underlying) to a risk-neutral measure (which is used to price options).

Transformation of a measure into an equivalent measure is known as a Girsanov transformation. The main ingredient in this transformation is the notion of the Radon-Nikodym derivative. Girsanov transforms are treated by e.g. Etheridge in [Ethe02, theorem 4.5.1 and theorem 7.3.5]. The Girsanov transform for the Black & Scholes model states that the drift and the Brownian motion of the process will change, whereas the volatility parameter stays the same. If we include jumps and get a jump diffusion model the intensity parameter will also change.

The jump diffusion model introduced above is not a complete model as there does not exist a unique equivalent measure. From the Girsanov transformation for jump diffusion models (see [Ethe02, theorem 7.3.5]) we see both the drift and intensity parameter will change, while the other parameters remain the same. However, the exact transform is specified by two unknown, so called change of measure, parameters. In the Black & Scholes model, containing only one such parameter, the parameter is found via the arbitrage argument discussed above leading to a drift r . With our assumption the drift parameter remains the same and only the intensity parameter will change during the Girsanov transformation.

In the literature several assumptions are made to come around the specification of the other change of measure parameter. The original jump diffusion model by Merton was specified by the assumption that jump risk is diversifiable. With this assumption he did assume that jump risk equals zero.

A different approach is to leave the concept of risk neutral pricing and to use risk based pricing. Often one assumes the martingale measure is optimal with respect to some (arbitrary) utility function. An utility function is the mathematical representation of the risk preferences of an investor. Which condition should be implemented is arguable. Examples include Lewis, who opts for the power utility function in [Lew01], Schweizer, who works on mean-variance hedging in [Schw92], and Kallsen, who opts for local utility in [Kall99]. Some support for the power utility function comes from Gerber & Shiu, who in [Shiu00] note the Esscher transform can be compared to a power utility function. If we apply the Esscher transform, the density process depends on the current price and not on the entire price history. Raible conjectures in [Raib00] the Esscher transform is under certain technical conditions in fact the only transformation which shows this behavior.

Also it is possible to calibrate the model to observable market prices. Taking a quoted option price, we can find the correct, or implied, jump intensity $\tilde{\lambda}$ according to the market. Barz proposes a method to use forward prices (see [Barz99, paragraph 5.2]) to find an implied intensity parameter. Using the forward dynamics one can avoid to model the effects of storage costs and convenience yield.

A new approach seems the idea of using an import option to calibrate the model. It acknowledges there is a possibility to flow electricity from one market to another. In the Netherlands it is for example possible to buy the right to import electricity from Germany. If the price difference between the markets is high enough, one can exercise the option. A drawback is that the transportation

channel is limited and arbitrage reasoning might be flawed.

Our approach will be to calibrate the model with a quoted option price. It avoids choosing an arbitrary utility function, acknowledges jump risk and is relatively easy to perform. For this purpose we looked at the most liquid option available on the Dutch spot electricity market, which has strike 30 and costs around Euro 2.50. With this the market tells us the long term option price equals $\frac{2.50}{30} \approx 0.08$.

Before we can correctly price the European put option, we will need to find a solution to our pricing problem stated in proposition 1. With a general solution and a correct estimation of the different parameters for our model, we can estimate the implied intensity $\tilde{\lambda}$. In the following chapter we take the first step and present two different numerical methods.

4 Numerical methods

In this section we discuss two methods to find a numerical solution to our pricing problem. Instead of the forward PIDE in (14), we will solve the equivalent backward PIDE in (21) given the initial condition in (15). For ease of presentation we assume for the remainder of this report the jump density function to be symmetric. In particular this means we take $p = q = \frac{1}{2}$ and $\eta \equiv \eta_1 = \eta_2$. Both described methods do not make use of this assumption and extend without any problem to other jump density functions. In the last paragraph we compare the two methods where Fourier expansion comes out as the better.

4.1 Fourier expansion

In a similar situation [Barz99, p. 21] conjectured a solution to the PIDE in (21) as in the following proposition:⁵

Proposition 2 *A solution to the PIDE is given by*

$$\psi(X_\tau, \tau) = e^{A(\tau) - X_\tau B(\tau)} \quad (22)$$

This set of solutions is due to the affine structure of our PIDE as noted by Duffie, Pan & Singleton in [Duff00]. Using the proposition it will be possible to find a solution to the PIDE. However, the boundary condition is a C^0 -function, while the proposed solution is a C^∞ -function. Thus the proposed solution does not obey the initial condition around the strike, which is taken to be 1. The approach we take here is based on a Fourier expansion of proposed solutions.

Let us first consider the convolution of the PIDE if $\psi(X_\tau, \tau)$ is of the form (22). We assume $-\eta < \text{Re}(B(\tau)) < \eta$ to make the convolution convergent with density function (13). Later we will show that this always holds. Combination of (13) and (19) with the assumption of a symmetrical jump density gives

$$\begin{aligned} K\psi(X_\tau, \tau) &= \frac{\lambda\eta}{2} e^{A(\tau) - X_\tau B(\tau)} \left(\int_{-\infty}^0 e^{(\eta - B(\tau))y} dy + \int_0^\infty e^{-(\eta + B(\tau))y} dy \right) \\ &= \frac{\lambda\eta^2}{\eta^2 - B^2(\tau)} \psi(X_\tau, \tau) \end{aligned} \quad (23)$$

The partial derivatives of (22) with respect to x and τ , and the second order partial derivative with respect to x , are

$$\frac{\partial\psi}{\partial x} = -B(\tau)\psi(X_\tau, \tau) \quad (24)$$

$$\frac{\partial^2\psi}{\partial x^2} = B^2(\tau)\psi(X_\tau, \tau) \quad (25)$$

$$\frac{\partial\psi}{\partial\tau} = \left[\frac{\partial A(\tau)}{\partial\tau} - X_\tau \frac{\partial B(\tau)}{\partial\tau} \right] \psi(X_\tau, \tau) \quad (26)$$

⁵Note the conditional characteristic function given by Barz in his (3.54) does not satisfy the two equations coming from the Kolmogorov backward equation in his (3.52)

Substituting (23) and the partial derivatives in (24), (25) and (26) into the backward PIDE yields:

$$\begin{aligned} \psi(X_\tau, \tau) \left[-\frac{\partial A(\tau)}{\partial \tau} - \kappa \alpha^* B(\tau) + \frac{1}{2} \sigma^2 B^2(\tau) + \frac{\lambda \eta^2}{\eta^2 - B^2(\tau)} - \lambda \right] \\ + X_\tau \psi(X_\tau, \tau) \left[\kappa B(\tau) + \frac{\partial B(\tau)}{\partial \tau} \right] = 0 \end{aligned} \quad (27)$$

This equation should hold for all X_τ , which implies the part dependent on X_τ and the part independent on X_τ should both equal zero. This gives the following system

$$0 = -\frac{\partial A(\tau)}{\partial \tau} - B(\tau) \kappa \alpha^* + \frac{1}{2} \sigma^2 B^2(\tau) + \frac{\lambda \eta^2}{\eta^2 - B^2(\tau)} - \lambda \quad (28)$$

$$0 = \kappa B(\tau) + \frac{\partial B(\tau)}{\partial \tau} \quad (29)$$

Equation (29) can be integrated yielding, with integration constant q_1 ,

$$B(\tau) = q_1 e^{-\kappa \tau} \quad (30)$$

Inserting (30) into (28) and integrating gives, with integration constant q_2 ,

$$\begin{aligned} A(\tau) = & \frac{\sigma^2 \eta^2}{4\kappa} \left[\frac{1}{2} \ln(B^2(\tau) - \eta^2) - \ln(q_1 - \eta e^{\kappa \tau}) - \ln(q_1 + \eta e^{\kappa \tau}) \right] \\ & + \alpha^* B(\tau) - \frac{\sigma^2}{4\kappa} B^2(\tau) + \frac{\lambda}{2\kappa} \ln(\eta^2 e^{2\kappa \tau} - q_1^2) - \lambda \tau + q_2 \end{aligned} \quad (31)$$

With these closed form expressions for $A(\tau)$ and $B(\tau)$ we have verified the proposition on the form of a solution to the PIDE.

The next step is to Fourier expand the boundary condition in terms of solutions to the PIDE. The Fourier series in complex form of a function $f \in C^\infty(\overline{\Omega})$ a.e. (that is: f is almost everywhere differentiable and defined on a closed interval Ω) defined as:

$$\sum_{n=-\infty}^{\infty} c_n e^{\frac{-2\pi n x}{L} i} \quad (32)$$

with

$$c_n = \frac{1}{L} \int_{-\frac{L}{2}}^{\frac{L}{2}} f(x) e^{\frac{2\pi n x}{L} i} dx \quad (33)$$

Two important characteristics of a Fourier series are that it is unique and converges uniformly with respect to the norm of $L^2(\overline{\Omega})$, see [Simo83, p. 447]. To

facilitate a Fourier expansion, integration constant q_1 in (30) is chosen to be purely imaginary (compare to (33)) as follows:

$$q_1(n) = \frac{2\pi n}{L}i \quad (34)$$

Note the real part of $B(\tau)$ equals zero and the assumption $-\eta < \text{Re}(B(\tau)) < \eta$ holds for all τ . Integration constant q_2 in (31) is determined by imposing the following condition

$$A(0) = 0 \quad (35)$$

Note this condition sets the complex phase of (22) to zero at $\tau = 0$:

$$\psi(X_\tau, 0) = e^{-q_1(n)X_\tau}$$

We define $\psi_n(X_\tau, \tau)$ to be a solution to the backward PIDE with the given choices (34) and (35). To find a solution we define (compare to (32))

$$\psi(X_\tau, \tau) = \sum_{n=-\infty}^{\infty} c_n \psi_n(X_\tau, \tau) \quad (36)$$

By the superposition principle (the differential and convolution operators are linear) the function $\psi(X_\tau, \tau)$ in (36) satisfies the backward PIDE in (21). By construction it also satisfies the initial condition (15) and we conclude equation (36) offers a closed form solution to our pricing problem stated in proposition 1. The constants c_n become in our case

$$\begin{aligned} c_n &= \frac{1}{L} \int_{-\frac{L}{2}}^{\frac{L}{2}} \psi(x, 0) e^{q_1(n)x} dx = \frac{1}{L} \int_{-\frac{L}{2}}^0 (1 - e^x) e^{q_1(n)x} dx \\ &= \frac{1}{L} \left[\frac{1}{q_1(n)} (1 - e^{-\frac{q_1(n)L}{2}}) - \frac{1}{1 + q_1(n)} (1 - e^{-\frac{(1+q_1(n))L}{2}}) \right] \end{aligned} \quad (37)$$

Finally, note the solution we find is a real number as the imaginary parts in term n and $-n$ cancel each other during the summation in (36). Let us write $\psi_n(x_\tau, \tau) \equiv \exp(\beta_1 + in\beta_2)$ and $c_n \equiv \rho_1 + i\rho_2$ to see the cancellation:

$$\begin{aligned} c_n \psi_n + c_{-n} \psi_{-n} &= c_n \beta_1 [\cos(n\beta_2) + i \sin(n\beta_2)] + \overline{c_n} \beta_1 [\cos(n\beta_2) - i \sin(n\beta_2)] \\ &= 2\beta_1 [\rho_1 \cos(n\beta_2) - \rho_2 \sin(n\beta_2)] \end{aligned}$$

where $\overline{c_n}$ denotes the complex conjugate of c_n .

If we want to find a practical solution to our PIDE-problem we will sum a finite number instead of an infinite number of terms. We have found 250 terms were enough to get good convergence with the following parameters: $\eta = 15$, $\kappa = 0.20$, $\sigma = 0.090$, $\alpha = 3.33$, $\lambda = 1.67$.

In the last paragraph of this section we show more results of applying this method. First, we will discuss another way to find a numerical solution.

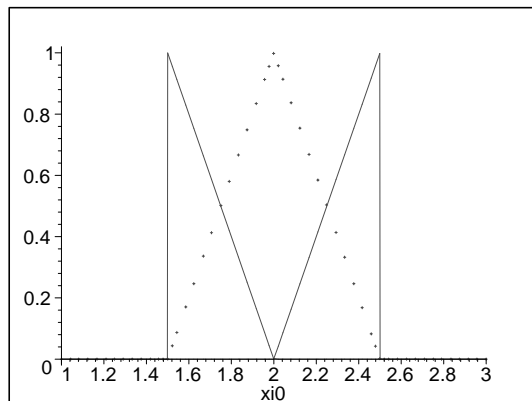


Figure 4: The cell centered at $\xi = 2$ with $\delta = 1$. Function $p^{(1)}$ is the line from $(1.5, 1)$ to $(2, 0)$, function $p^{(2)}$ is the dotted rooftop intersecting $(2, 1)$ and function $p^{(3)}$ is the line from $(2, 0)$ to $(2.5, 1)$.

4.2 Finite Difference - Finite Elements

In the foregoing subsection we have shown a way to find a closed form solution to the PIDE in (21) by means of Fourier expansion. That solution is due to the assumption of a very special form of the double exponential jump density. In this subsection we discuss an approach, which works for more general cases. The method is based upon approximation of the time derivative with the Finite Difference method in combination with the Finite Elements method.

The first step in our approach is to use the Finite Difference method. In this method one discretizes time in small intervals of length $d\tau$, such that time derivatives can be approximated. Starting from the known solution (the initial condition) on time level $\tau = 0$, we can make a time step to time level $d\tau$ and so forth. For a given $d\tau$ we approximate the partial derivative with respect to time as

$$\frac{\partial\psi(x, \tau)}{\partial\tau} \approx \frac{\psi(x, \tau) - \psi(x, \tau - 1)}{d\tau} \quad (38)$$

Note that better approximations like the Crank-Nicholson approximation are available, but we use this ‘easy’ approximation. An advanced Finite Difference method has been applied to a jump diffusion model by Andersen & Andreasen. They address the case of log-normal jumps for which they find a numerical solution by means of the Alternating Directions Implicit (or ADI) method. We refer the interested reader to their paper [Ande02, par 3.1] for a description of this method.

Using approximation (38) we can rewrite the backward PIDE in (21) into

$$d\tau(L + K)\psi(x, \tau) - \psi(x, \tau) = -\psi(x, \tau - 1) \quad (39)$$

The next step in our approach is to use the Finite Elements method. Let us first introduce some notation. We look for a solution to (39) for a symmetrical

interval in x around 0 of total length $2Q$ (also called: computational window). The computational window is divided in N ‘cells’ of length δ , thus $\delta = \frac{2Q}{N}$. Each cell contains by construction three different linear splines, see for an illustration figure 4. A linear spline is a rooftop function of amplitude 1 with compact support, meaning the function differs from 0 only on a closed and finite interval (here of length δ). We define ξ_n to be the center of cell number n and denote an inner product by $\langle \cdot | \cdot \rangle$.

The three linear splines in cell number n are named basis functions $p^{(\cdot)}$ and defined as follows

- $p^{(1)}(x, \xi_n, \delta)$: linear spline centered at $\xi_n - \frac{\delta}{2}$
- $p^{(2)}(x, \xi_n, \delta)$: linear spline centered at ξ_n
- $p^{(3)}(x, \xi_n, \delta)$: linear spline centered at $\xi_n + \frac{\delta}{2}$

We give the name test function, denoted by $\Xi(x, \xi_c, \delta)$, to the linear spline centered at ξ_c .

The three basis functions can be represented as:

$$p^{(1)}(x, \xi_n, \delta) = \left[H(\xi_n - x) - H(\xi_n - x + \frac{\delta}{2}) \right] \frac{\xi_n - x}{\frac{\delta}{2}} \quad (40)$$

$$\begin{aligned} p^{(2)}(x, \xi_n, \delta) &= \left[H(\xi_n - x + \frac{\delta}{2}) - H(\xi_n - x) \right] \frac{\xi_n - x + \frac{\delta}{2}}{\frac{\delta}{2}} \\ &+ \left[H(\xi_n - x - \frac{\delta}{2}) - H(\xi_n - x) \right] \frac{\xi_n - x - \frac{\delta}{2}}{\frac{\delta}{2}} \end{aligned} \quad (41)$$

$$p^{(3)}(x, \xi_n, \delta) = \left[H(\xi_n - x) - H(\xi_n - x - \frac{\delta}{2}) \right] \frac{\xi_n - x}{\frac{\delta}{2}} \quad (42)$$

where $H(x)$ denotes the Heaviside function defined by

$$H(x) = \begin{cases} 0 & \text{if } x \leq 0 \\ 1 & \text{if } x > 0 \end{cases}$$

Taking the inner product of test function $\Xi(x, \xi_c, \delta)$ with (39) gives

$$\langle d\tau L\psi(x, \tau) - \psi(x, \tau) | \Xi \rangle + \langle d\tau K\psi(x, \tau) | \Xi \rangle = - \langle \psi(x, \tau - 1) | \Xi \rangle \quad (43)$$

Our approach is based on the compact support of the test function together with the following approximation theorem:

Theorem 2 *A linear combination in each cell of the three basis functions $p^{(\cdot)}$ defined above with amplitudes $a^{(\cdot)}$, approximates the solution $\psi(x, \tau)$ in the whole computational window as*

$$\psi(x, \tau) = \sum_{n=1}^N \sum_{j=1}^3 a^{(j)} p^{(j)}(x, \xi_n, \delta) \quad (44)$$

More insight in this theorem can be found in [Pete98] or [Simo83].

Now let us start by finding expressions for the inner product of the different operators with the test function. By integration by parts the second order partial derivative in L in (18) becomes, due to the compact support of $\Xi(x, \xi_c, \delta)$,

$$\begin{aligned}
\int_{-\infty}^{\infty} \Xi(x, \xi_c, \delta) \frac{\sigma^2}{2} \frac{\partial^2 \psi}{\partial x^2} dx &= \int_{\xi_c - \frac{\delta}{2}}^{\xi_c + \frac{\delta}{2}} \Xi(x, \xi_c, \delta) \frac{\sigma^2}{2} \frac{\partial^2 \psi}{\partial x^2} dx \\
&= \left[\phi_0(x) \frac{\sigma^2}{2} \frac{\partial \psi}{\partial x} \right]_{\xi_c - \frac{\delta}{2}}^{\xi_c + \frac{\delta}{2}} - \frac{\sigma^2}{2} \int_{\xi_c - \frac{\delta}{2}}^{\xi_c + \frac{\delta}{2}} \frac{\partial \Xi(x, \xi_c, \delta)}{\partial x} \frac{\partial \psi}{\partial x} dx \\
&= -\frac{\sigma^2}{2} \int_{\xi_c - \frac{\delta}{2}}^{\xi_c + \frac{\delta}{2}} \frac{\partial \Xi(x, \xi_c, \delta)}{\partial x} \frac{\partial \psi}{\partial x} dx \tag{45}
\end{aligned}$$

Note the partial derivative of $\psi(x, \tau)$ with respect to x reduces in the interval $(\xi_c - \frac{\delta}{2}, \xi_c + \frac{\delta}{2})$ to

$$\frac{\partial \psi}{\partial x} = \frac{\partial}{\partial x} \sum_{n=1}^N \sum_{j=1}^3 a_n^{(j)} p^{(j)}(x, \xi_n, \delta) = \sum_{j=1}^3 a_c^{(j)} \frac{\partial p^{(j)}(x, \xi_c, \delta)}{\partial x} \tag{46}$$

Using (46) we can simplify equation (45) to

$$\int_{-\infty}^{\infty} \Xi(x, \xi_c, \delta) \frac{\sigma^2}{2} \frac{\partial^2 \psi}{\partial x^2} dx = \frac{\sigma^2}{\delta} \left(a_c^{(1)} - 2a_c^{(2)} + a_c^{(3)} \right) \tag{47}$$

Due to the compact support of $\Xi(x, \xi_c, \delta)$ the first order partial derivative in L is equal to

$$\int_{\xi_c - \frac{\delta}{2}}^{\xi_c + \frac{\delta}{2}} p^{(m)}(x, \xi_c, \delta) \kappa (\alpha^* - x) \frac{\partial \psi}{\partial x} dx \tag{48}$$

which can be simplified to

$$\left(\frac{\kappa}{2} \xi_c - \frac{\kappa}{12} \delta - \frac{\kappa \alpha^*}{2} \right) a_c^{(1)} + \frac{\delta \kappa}{6} a_c^{(2)} + \left(\frac{\kappa}{2} \xi_c + \frac{\kappa}{12} \delta - \frac{\kappa \alpha^*}{2} \right) a_c^{(3)} \tag{49}$$

Due to the compact support of $\Xi(x, \xi_c, \delta)$ the zero order partial derivative in L is equal to

$$\int_{\xi_c - \frac{\delta}{2}}^{\xi_c + \frac{\delta}{2}} p^{(m)}(x, \xi_c, \delta) (-\lambda \psi) dx \tag{50}$$

which can be simplified to

$$-\frac{\delta \lambda}{12} \left(a_c^{(1)} + 4a_c^{(2)} + a_c^{(3)} \right) \tag{51}$$

Combining equations (47), (49) and (51) leads to

$$\begin{aligned}
\langle d\tau L\psi - \psi | \Xi(x, \xi_c, \delta) \rangle &= \left(\frac{\kappa d\tau}{2} \xi_c - \frac{\kappa \alpha^* d\tau}{2} + \frac{\sigma^2}{\delta} - \frac{\delta}{12} (1 + \kappa d\tau + \lambda d\tau) \right) a_c^{(1)} \\
&+ \left(-\frac{\delta}{3} (1 + \lambda d\tau) + \frac{\kappa \delta d\tau}{6} - \frac{2\sigma^2}{\delta} \right) a_c^{(2)} \\
&+ \left(-\frac{\kappa d\tau}{2} \xi_c + \frac{\kappa \alpha^* d\tau}{2} + \frac{\sigma^2}{\delta} \right) a_c^{(3)} \\
&- \frac{\delta}{12} (1 + \kappa d\tau + \lambda d\tau) a_c^{(3)} \tag{52}
\end{aligned}$$

The inhomogeneous term is similar to (50) with time $\tau-1$. Thus (51) implies the inner product is given by

$$-\langle \psi(x, \tau-1) | \Xi(x, \xi_c, \delta) \rangle = -\frac{\delta}{12} \left(a_c^{(1), \tau-1} + 4a_c^{(2), \tau-1} + a_c^{(3), \tau-1} \right) \tag{53}$$

Owing to the convolution which couples all cells to each other, we have to take more than three splines into account to obtain $\langle K\psi | \Xi(x, \xi_c, \delta) \rangle$.

Combining (19) and (44) we get:

$$\begin{aligned}
\lambda \int \psi(y, \tau) f_Y(y-x) dy &= \frac{\lambda}{2} \int_{-\infty}^x \eta e^{\eta(y-x)} \sum_{n=1}^N \sum_{j=1}^3 a_n^{(j)} p^{(j)}(y, \xi_n, \delta) dy \\
&+ \frac{\lambda}{2} \int_x^{\infty} \eta e^{-\eta(y-x)} \sum_{n=1}^N \sum_{j=1}^3 a_n^{(j)} p^{(j)}(y, \xi_n, \delta) dy \tag{54}
\end{aligned}$$

By interchanging the order of integration and summation the convolution becomes

$$\sum_{n=1}^N \frac{\lambda}{2} \left[\int_{-\infty}^x \eta e^{\eta(y-x)} \sum_{j=1}^3 a_n^{(j)} p^{(j)}(y, \xi_n, \delta) dy + \int_x^{\infty} \eta e^{-\eta(y-x)} \sum_{j=1}^3 a_n^{(j)} p^{(j)}(y, \xi_n, \delta) dy \right] \tag{55}$$

In appendix A we give the expression for the convolution dependent on the relation between x , δ and ξ_n . From (73), (74), (75) and (76) in the appendix one can see the convolution is a sum of factors which get smaller in exponential speed with the distance between the position of the observation point x compared to the center of the segment ξ_n . We show also in appendix A how to find the correct formulas for the inner product of the convolution with the test function $\Xi(x, \xi_c, \delta)$.

Note, that the linear splines which are available in two cells, $p^{(1)}$ and $p^{(3)}$, are counted double in the summation of (44). The best way to circumvent this is to solve the problem by looking at the spline amplitudes of all available linear splines.

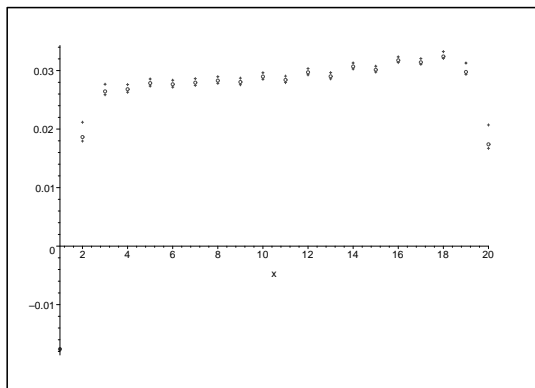


Figure 5: Difference between FDFE and Fourier for $N = 20$ (top), $N = 40$ (middle) and $N = 60$ (bottom)

Looking in the cell with center ξ_c , we get from (52) and (53) spline amplitudes in that cell. The convolution couples all cells, such that the left hand side of (43) becomes a function of the spline amplitudes of all linear splines in the computational window. The right hand side of (43) is by assumption a known value for all values in the computational window. In total there are $2N + 1$ spline amplitudes, such that we need $2N + 1$ equations to solve for them.

This can be done by looking exactly in the center of the $2N + 1$ linear splines. We can derive an equation in each center leading to a set of $2N + 1$ equations. For this kind of linear problems there are specialized solvers available. However, the involved matrix is dense due to the convolution and matrix inversion takes lot of CPU time. To give an indication of CPU time: in Maple this inversion takes 10 seconds for $N = 20$ and 3 hours for $N = 80$.

After matrix inversion the solution is known for time level $d\tau$ and we can make another iteration. In the following subsection we will compare both presented numerical methods.

4.3 Numerical results

In this section we have developed two different ways to find a numerical solution to the PIDE. We have implemented both algorithms, which are used to make a comparison between the methods and to discuss sensitivity in the option price for the different parameters.

In the Finite Difference - Finite Elements (shortly FDFE) method we have used two discretization parameters: time step $d\tau$ and amount of cells N . One would expect the discretization error becomes smaller if we use more cells or use a smaller time step. In the Fourier expansion method we find convergence increasing the amount of terms included.

A comparison between both the methods is done in figure 5 where we were interested if both methods converge to the same value. The Fourier expansion

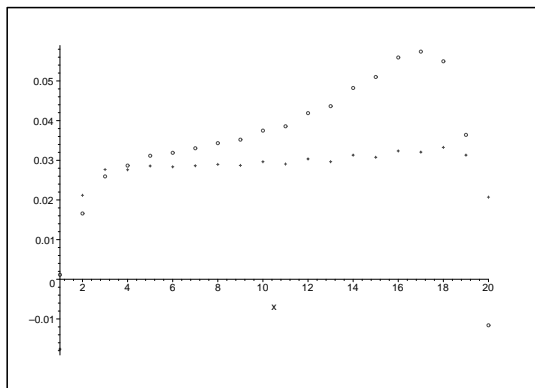


Figure 6: Difference between FDFE and Fourier for 1 time step $d\tau = 0.01$ (diamond) and 5 time steps of $d\tau = 0.002$ (circle)

method is used as a base and we see the FDFE method is having an error of about 0.025. If we increase N from 20 to 40 to 60, we observe the difference decreases, but it will not disappear with a feasible computational time.

Another way to find better results in the FDFE method is to decrease the time step by a factor $1/q$ and then iterate q time steps. In figure 6 we show the result of taking 5 time steps of $d\tau = 0.002$ instead of 1 timestep of $d\tau = 0.01$. Instead of getting a better match, the difference gets bigger and doesn't disappear if we increase N : FDFE produces an unstable result.

We believe thus the FDFE is not appropriate for this parameter set. Changing the parameter set does not give better results, leading to the conclusion the Fourier expansion method is our preferred method. Possible reasons for this include a too simple finite difference approach in (39) and / or too low amount of segments N and / or too high time step.

In the remaining of this paragraph we will use the Fourier expansion method to do a sensitivity analysis. Let us first remember that we should change the intensity parameter λ according to the Girsanov transformation as discussed in paragraph 3.4 to find a correct option price. From the most liquid option available on the Dutch spot electricity market, we estimated the long term option price equals $\frac{2.50}{30} \approx 0.08$. Assuming the other parameters are given by $\sigma = 0.050$, $\kappa = 0.26$, $\alpha^* = 3.30$ and $\eta = 12$, we have an implied $\tilde{\lambda} = 0.20 \cdot 10^3$. These parameters are found in the following section, where we will do the parameter estimation. Comparing with the estimated parameter $\lambda = 4.27$ in table 1, one can say the increase is huge.

With these parameters (including $\tilde{\lambda}$) we have plotted in figure 7 the option price $\psi(X_\tau, \tau)$ against X_τ for several time levels: $\tau = \{0, 1, 2, 3, 4, 8\}$. For $\tau = 0$ there is a pay-off for $x < 0$ like $1 - e^x$ and no value otherwise. If there is time to maturity there is a chance the in-the-money option might end up out-of-the-money leading to a lower option price. In the graph we observe this decrease in the option price if time to maturity increases. Eventually this will lead to a

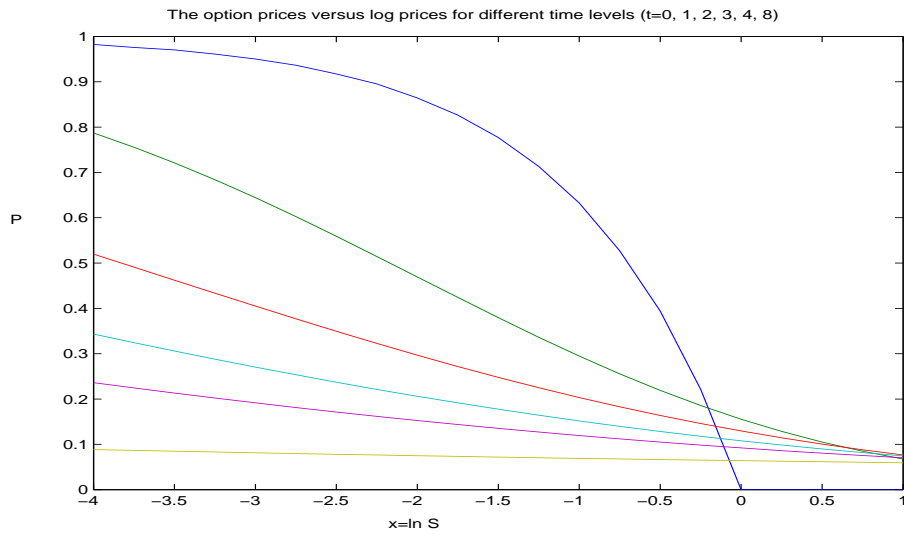


Figure 7: Option price plotted against x

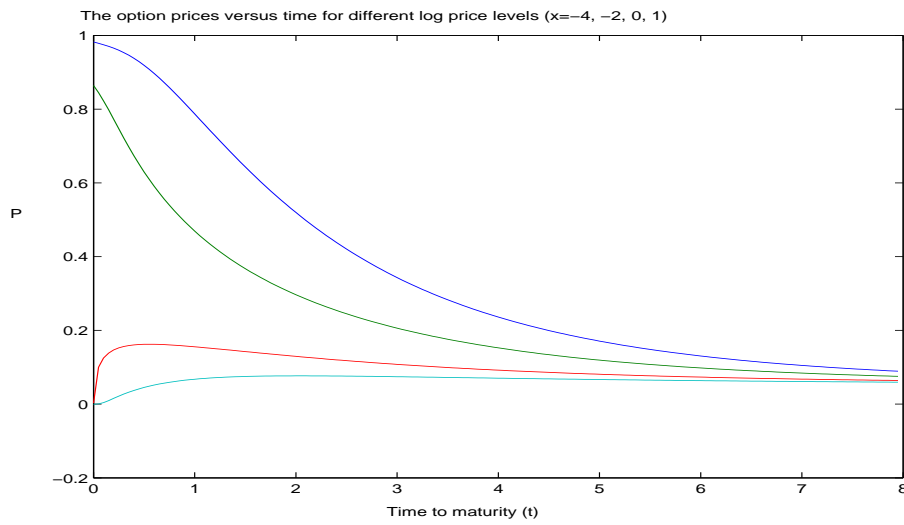


Figure 8: Option price plotted against τ

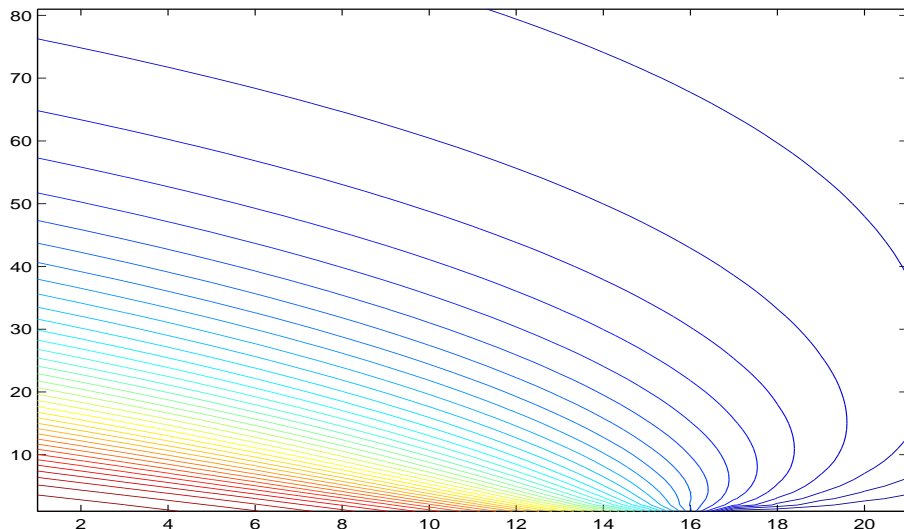


Figure 9: Contour plot: the lines show combinations of (X_t, τ) which lead to the same option price

horizontal line representing the long term option price.

In figure 8 the option price $\psi(X_\tau, \tau)$ is plotted against τ for several logged spot electricity prices X_τ . In the graph we see the option prices are similar after one week regardless today's spot electricity price. Up to one week the value can change significantly. The same problem with pricing long term options under a jump diffusion model was noted by Barz in [Barz99]. His option prices converged in a few weeks, while ours converged in a week. Main reason seems to be that his λ is an order of magnitude 10 bigger.

If we want to observe both the influence of changing time and changing the logged spot electricity price X_τ , we can instead look at contour plots. In figure 9 we give 40 contour plots for the same parameters as before containing the prices in the range of 0...4. The price difference between two contours is set to 0.1. If we are at maturity, that is the horizontal axis, there is only a pay-off for negative values of x . For positive x we see a time-value, which for small τ disappears. The 'boomerang'-shape on the right hand side is hard to explain economically. Coming towards maturity the option price can both increase and decrease, dependent on the exact time to maturity. Barz encountered the same phenomenon in [Barz99, figure 5.2], but unfortunately did not mention any explanation. We investigated it by putting $\lambda = 0$ where the boomerang disappeared. So we believe the shape comes into existence with the introduction of jumps.

To see the reaction to a change in the parameters, we have lowered the parameters *ceteris paribus* (that is: keeping the other parameters constant) to $\lambda = 50$ in figure 10, $\kappa = 0.20$ in figure 11, $\eta = 10$ in figure 12 and $\sigma = 0.010$ in

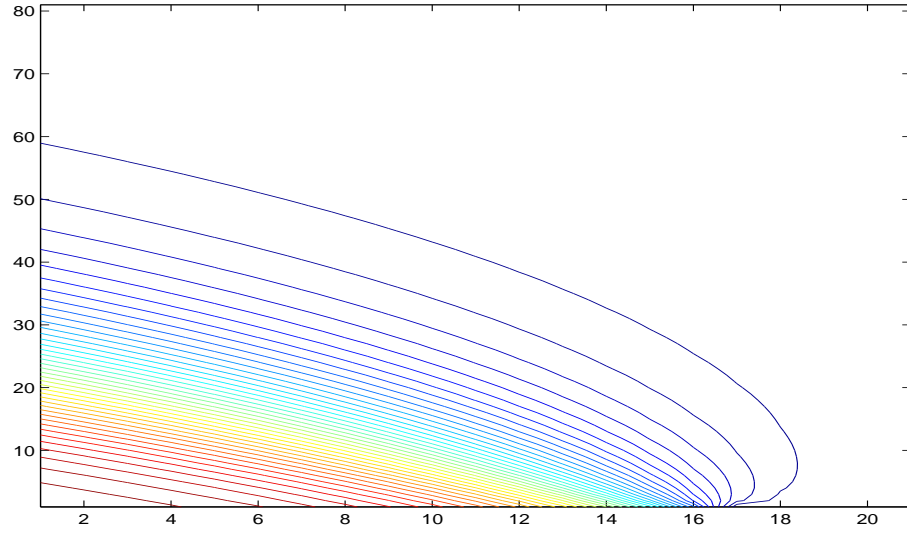


Figure 10: Contour plot for reduced λ : the lines show combinations of (X_τ, τ) which lead to the same option price.

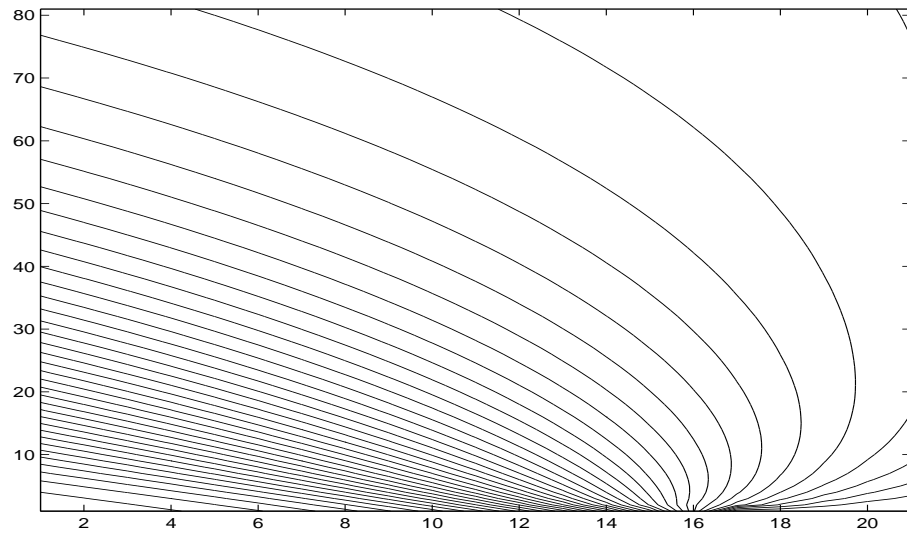


Figure 11: Contour plot for reduced κ : the lines show combinations of (X_τ, τ) which lead to the same option price.

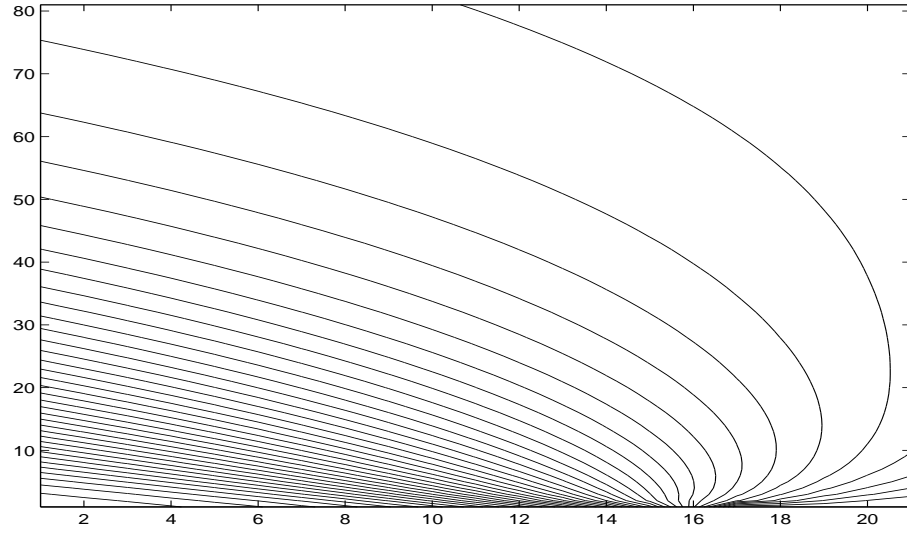


Figure 12: Contour plot for reduced η : the lines show combinations of (X_τ, τ) which lead to the same option price.

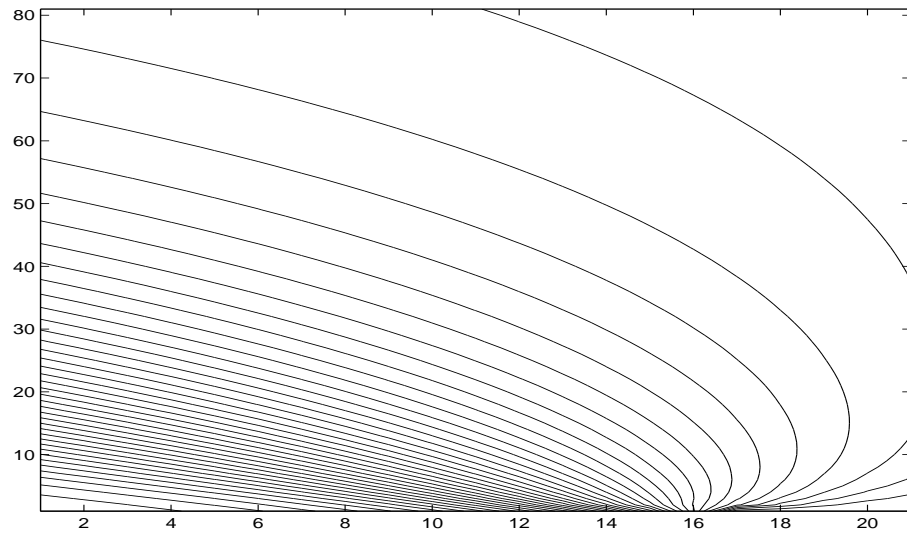


Figure 13: Contour plot for reduced σ : the lines show combinations of (X_τ, τ) which lead to the same option price.

figure 13.

An interesting result is figure 13, which is very alike figure 9: a change in σ hardly affects the option price. Though one would expect a small decrease in diffusion, it turns out the very large λ (compared to σ) dominates the option price. A decrease in κ implies spot electricity prices are pulled back less and leads thus to a higher diffusion. A decrease in η implies the jump density is less centered around its mean and we expect more diffusion. A decrease in λ implies less frequent jumps and thus less diffusion.

5 Parameter estimation

In the double exponential jump diffusion model we have introduced five different parameters: mean-reversion coefficient κ , drift coefficient α^* , volatility σ of the Brownian motion, decay parameter of the jump diffusion η and jump intensity parameter λ . Our goal in this chapter is to estimate these parameters.

5.1 Different estimation methods

In the literature several methods to estimate parameters of a continuous time stochastic process have been proposed. Within statistical analysis the maximum likelihood (ML) estimation is a preferred method, because it is consistent and asymptotically efficient. In this method one tries to maximize the likelihood of obtaining the real time-series. The ML estimators are those parameters, which maximize the likelihood function (or joint density function) of the obtained sample.

In a similar setup Barz in [Barz99, paragraph 3.4] has used ML to estimate parameters for a jump diffusion model. Given a set of parameters, he derives the conditional characteristic function and uses the Fourier inversion formula to numerically determine the conditional density function. The conditional density function serves as an input for the ML-estimation. He solves for the parameters by iteration.

We refrain from his method for two reasons. In the first place one needs much CPU-time as each iteration step includes numerical evaluation of an inverse Fourier transform. In the second place we think this estimation method might lead to more than one local maximum for each parameter.

Another approach, known as the empirical characteristic function (or ECF) method, matches instead characteristic functions. Jiang and Knight describe in [Jian00] an approach based on the unconditional joint characteristic function, while Singleton in [Sing01] uses the conditional characteristic function. The idea behind this method is to determine a theoretical characteristic function and match it to the empirical characteristic function.

The ECF method is close to the Method of Moments (or MoM) approach. In MoM one matches the first moments of the process, while the ECF method matches all moments of the process. We have decided to apply the ECF method to estimate our parameters.

5.2 Theoretical conditional characteristic function

Let us introduce the characteristic function of X_T conditional on filtration F_t as

$$\phi(X_t, t, T, k) = \mathbf{E}(e^{ikX_T} | X_t) \quad (56)$$

It is possible, under technical regularity conditions, to characterize the form of the conditional characteristic function as shown by Duffie, Pan & Singleton in [Duff00, proposition 1]. If we follow Heston's derivation of the characteristic function in [Hest93, appendix] (i.e. apply Ito's formula to a general conditional

expectation to find a Fokker-Planck equation and connect it to the conditional characteristic function) we can find the exact characterization. The following theorem brings together these two results

Theorem 3 *The characteristic function is of the following form*

$$\phi(X_t, t, T, k) = \exp(A(t) - X_t B(t)) \quad (57)$$

It satisfies, with L and K introduced in (18) and (19), the Kolmogorov backward equation

$$(L + K)\phi(X_t, t, T, k) + \frac{\partial \phi(X_t, t, T, k)}{\partial t} = 0 \quad (58)$$

with the terminal conditions

$$A(T) = 0 \quad (59)$$

$$B(T) = -ik \quad (60)$$

Finding the conditional characteristic function for the jump diffusion model, can thus be compared to the situation we encountered in the foregoing subsection. In (22) we conjectured a solution similar to (57) to the option backward PIDE in (21), which is exactly the same PIDE as (58). Using the same boundary conditions as (59) and (60) we found an expression for $B(t)$ in (30) and for $A(t)$ in (31).

There is only a subtle difference between the option pricing problem and the conditional characteristic function in the terminal conditions. Note, that the conditional characteristic function must satisfy the boundary conditions (59) and (60), while we chose the same conditions for the option price in order to facilitate a Fourier expansion.

For completeness let us state the conditional characteristic function resulting from theorem 3:

Theorem 4 *The conditional characteristic function of random variable X_T is given by*

$$\phi(X_t, t, T, k) = \exp\left(A(t) + ike^{-\kappa(T-t)} X_t\right) \quad (61)$$

where

$$\begin{aligned} A(t) &= \frac{k^2 \sigma^2}{4\kappa} (e^{-2\kappa(T-t)} - 1) + \frac{\lambda}{2\kappa} \left[\ln(\eta^2 e^{2\kappa(T-t)} + k^2) - \ln(\eta^2 + k^2) \right] \\ &- \lambda(T-t) - i\alpha^* k (e^{-\kappa(T-t)} - 1) \end{aligned} \quad (62)$$

Before we continue, let us check the conditional characteristic function by the correspondence principle. We derive the conditional characteristic function for three special cases and compare them successfully with a reduced version of (61).

From the definition in (56) we see the characteristic function for $k = 0$ is

$$\phi(X_t, t, T, 0) = 1 \quad (63)$$

For $k = 0$ we get $A(t) = 0$ and equation (61) reduces to 1.

The special case $(\eta, \lambda) = \underline{0}$ is a mean reverting Brownian motion, which we denote by $X_t^{(1)}$. Since $X_T^{(1)}$ is a normally distributed random variable and thus determined totally by its expectation and variance, the conditional characteristic function of $X_T^{(1)}$ is given by

$$\phi(X_t, t, T, k)|_{(\eta, \lambda) = \underline{0}} = \exp\left(-\frac{k^2}{2} \text{var}\left(X_T^{(1)}\right) + ik\mathbf{E}\left(X_T^{(1)}\right)\right) \quad (64)$$

To find the expectation and variance, we can use [Bjor98, lemma 3.15, proposition 4.3], which yields

$$\mathbf{E}\left(X_T^{(1)}\right) = \alpha^* + (x_t - \alpha^*) e^{-\kappa(T-t)} \quad (65)$$

$$\text{var}\left(X_T^{(1)}\right) = \frac{\sigma^2}{2\kappa} \left(1 - e^{-2\kappa(T-t)}\right) \quad (66)$$

Combination of (64), (65) and (66) gives the same as reducing equation (61):

$$\phi(X_t, t, T, k)|_{(\eta, \lambda) = \underline{0}} = \exp\left(-\frac{k^2\sigma^2}{4\kappa} \left(1 - e^{-2\kappa(T-t)}\right) + ik\left[\alpha^* + (x_t - \alpha^*) e^{-\kappa(T-t)}\right]\right) \quad (67)$$

The final special case we consider is $(\kappa, \alpha, \sigma) = \underline{0}$, which is a pure jump process. If we take $x_t = 0$ and use the Lévy-Khintchine formula (see for example [Bert96]), the conditional characteristic function is:

$$\phi(X_t, t, T, k)|_{(\kappa, \alpha, \sigma) = \underline{0}} = \exp\left(\int_{-\infty}^{\infty} \lambda(T-t)(e^{ikm} - 1)f_Y(m)dm\right) \quad (68)$$

where $f_Y(m)$ is the density function given by (13). If we assume, as before, $p = q = \frac{1}{2}$ and $\eta \equiv \eta_1 = \eta_2$, substituting the density function into the integral gives:

$$\phi(X_t, t, T, k)|_{(\kappa, \alpha, \sigma) = \underline{0}} = \exp\left(-\frac{\lambda(T-t)k^2}{\eta^2 + k^2}\right) \quad (69)$$

This equation also comes out from a reduction in (61).

5.3 Empirical characteristic function

To create an empirical characteristic function, we use data series from the Dutch spot electricity market APX. We use the daily average APX price from January 2001 to July 2002 in order to avoid the daily pattern as we have seen in figure 3c. As we mentioned in chapter 1, the market was partially regulated before January 2001 with totally different market behavior from the regulated market. This led us to the choice of using data starting January 2001. The time step is thus $\Delta t = 1$ day implying all parameters will be estimated per day.

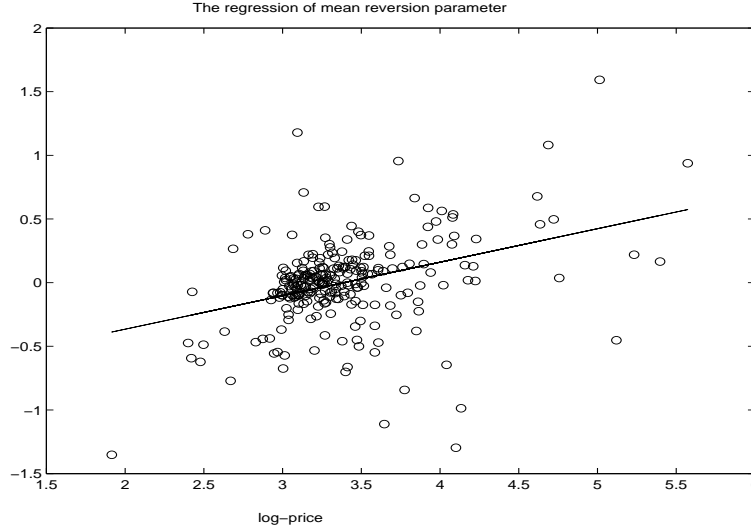


Figure 14: Scatter plot for APX baseload: difference of consecutive log APX prices versus log APX price

Transforming the SDE in (12) via $X_t = \ln S_t$, shows the expected value of dX_t , denoted by $\mathbf{E}(dX_t)$, satisfies

$$\mathbf{E}(dX_t) = \kappa(\alpha^* - X_t)dt \quad (70)$$

This equation shows a linear regression between the difference of consecutive logarithmic prices dX_t and the logarithmic price X_t , will yield an estimate for both κ and α^* . In figure 14 we show a scatter plot together with our regression line. From the figure it is clear we get a stable estimate of α^* (3.39) and an unstable estimate of κ (0.262).

Now let us look at the conditional density function, which can be found via the Fourier inversion formula (see e.g. [Duff00, equation (1.4)])

$$p(X_{t+1}|X_t) = \frac{1}{\pi} \int_0^\infty e^{-ikX_{t+1}} \phi(X_t, t, t+1, k) dk \quad (71)$$

Inserting the functional form of $\phi(X_t, t, t+1, k)$ from (61) gives

$$p(X_{t+1}|X_t) = \frac{1}{\pi} \int_0^\infty \exp(A(t) - ik[X_{t+1} - e^{-\kappa} X_t]) dk \quad (72)$$

where the dependency on $X_{t+1} - e^{-\kappa} X_t$ is clear (see also the remark at the end of this section.)

Given the value for κ , we have created the empirical characteristic function in the following steps:

- Given the time series of X_t and an estimate for κ , create the time series $X_{t+1} - e^{-\kappa} X_t$

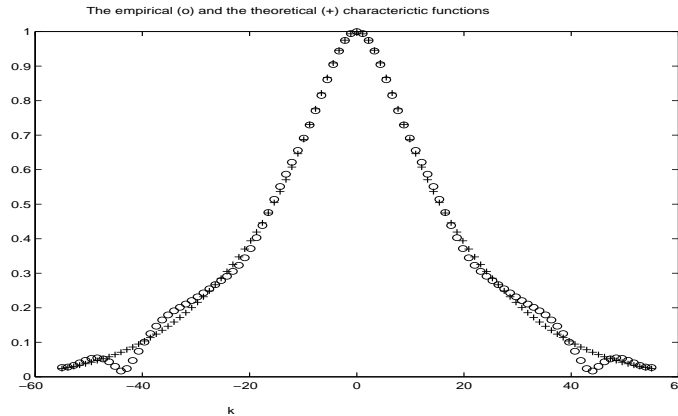


Figure 15: The absolute value of the empirical and matched theoretical characteristic function

- Determine a histogram by means of Matlab and assume this to be an approximation for the conditional density function $p(X_{t+1}|X_t)$
- Determine a conditional empirical characteristic function, denoted by $\phi(X_t, t, t + 1, k)$, via the definition:

$$\phi(X_t, t, t + 1, k) = \int_{-\infty}^{\infty} e^{ikX_{t+1}} p(X_{t+1}|X_t) dX_{t+1}$$

The three remaining parameters σ , η and λ are estimated by a naive minimization of the absolute difference between the empirical and theoretical characteristic function. We solve the following minimization problem:

$$\min_{\sigma, \eta, \lambda} \int_{-\infty}^{\infty} (|\phi^{em}(X_t, t, T, k)| - |\phi^{th}(X_t, t, T, k)|)^2 w(k) dk$$

where we have chosen weight function $w(k) \equiv 1$ for all k for convenience.

The Nelder-Meade simplex algorithm can solve this non-linear least squares problem and provides our parameter estimates. This specific algorithm is readily available in Matlab. In figure 15 we show the empirical and matched theoretical characteristic function for our data set. It can be seen the center is matched quite well, while the tails contain small errors. This can be attributed to the amount of points we used in the Fourier transformation. Taking a larger number results in a better fit. In table 1 we show our results of the parameter estimation.

The presented parameter estimation is a two step method. First one determines κ (at the same time leading to an estimate for α^*), which forms an input for the estimation of the remaining parameters.

To investigate the impact of κ , we have run the second step of the estimation for different κ . Instead of the correct estimation 0.262, we put in values 1.7 and

	α^*	κ	σ	λ	η
2001-2002	3.39	0.262	0.090	4.27	15.8

Table 1: Estimated parameters for daily average APX base load 01/2001-06/2002

2.7 and found the estimates are changing considerably. Remarkable is the drop in the error if κ increases. This might be attributed to the fact we have not chosen an optimal weight function in the minimization or to the fact we have a two step method.

κ	σ	λ	η	error
0.262	0.090	4.27	15.8	0.042
1.7	0.28	1.13	2.30	0.016
2.7	0.37	1.77	2.03	0.010

Table 2: Parameter estimates for different κ

Remark Note that taking logarithmic price differences to find a conditional density function only yields correct results for $\kappa = 0$. The moment one assumes a mean-reverting process, Value-At-Risk calculations should thus be based on the adjusted logarithmic price difference: $X_{t+1} - e^{-\kappa} X_t$.

6 Conclusion

Deregulated electricity supply markets are no longer unique in the world. Many countries already have, or are in the process towards, deregulating their electricity market. In this report we took the Dutch spot electricity market as an example and show prices behave different since deregulation. We find mean reversion and jumps are two important characteristics of the prices.

Describing spot electricity prices in a model gives insight in the risks involved in energy trading and shows a way to value electricity contracts. From the proposed models in the literature, we believe jump diffusion models and regime switching are most tractable. In this report we extended the double exponential jump diffusion model originally due to Kou & Wang in [Kou01] with mean-reversion.

We use this model to value a European put option on the spot electricity market. First a pricing equation is derived in PIDE-form in (14). Because electricity is non-storable, one cannot use no-arbitrage arguments to value the option. There is no general way around this problem, which can be seen as a weak point of all jump diffusion models. We chose to work with a zero convenience yield to stress there is no risk free portfolio available. Moreover we decided to calibrate our model to the most liquid option in the APX market to avoid the choice of an arbitrary utilityfunction. This calibration is done by changing the estimated jump intensity parameter λ to an implied value. In our case the value changed dramatically from 4.27 to $0.20 \cdot 10^3$.

Fourier expansion gives a way to find a numerical solution to the PIDE in terms of five different parameters. We have tested Finite Difference - Finite Elements method, which however seems to be unstable. We estimate these parameters by matching the theoretical characteristic function to the empirical one in a two step procedure. First we estimate mean reversion parameter κ , which is then used as an input to the estimation of the other parameters.

We confirm a result by Barz that jump diffusion models seem not appropriate for pricing options longer than a few weeks out as the option price under these models converges quickly.

The given approach is not restricted to European put options. We believe it can be extended to incorporate a more complex pay-off as long as the Fourier transform of a pay-off exists, we will be able to price the European option. To value Asian and American options asks for additional research.

Inner product convolution and test function

In this appendix we give detailed expressions for the convolution given by (55) and its inner product with the test function $\Xi(x, \xi_c, \delta)$. Introducing different expressions for the convolution, reduces the length of the formula's and can help to gain computational speed.

Due to the different Heaviside functions in the basis functions, see (40), (41) and (42), it is worth considering four different regions of the convolution dependent on the position of the observation point x compared to the center of the segment ξ_n and width of the segment δ . We introduce $K\psi_1(x, \tau)$ to $K\psi_4(x, \tau)$ depending on the relation between x , δ and ξ_n as in

- For $x < \xi_n - \frac{\delta}{2}$

$$\begin{aligned} K\psi_1(x, \tau) &= -\sum_{n=1}^N \frac{\lambda}{2\eta\delta} (e^{-\eta(-x+\xi_n)} [-4a_n^{(1)} + 2a_n^{(2)} + 2a_n^{(3)}] \\ &+ e^{-\frac{\eta}{2}(\delta-2x+2\xi_n)} [2a_n^{(1)} - 2a_n^{(2)} - \eta\delta a_n^{(2)}] \\ &+ e^{\frac{\eta}{2}(\delta+2x-2\xi_n)} [2a_n^{(1)} - 2a_n^{(3)} + \eta\delta a_n^{(3)}]) \end{aligned} \quad (73)$$

- For $\xi_n - \frac{\delta}{2} < x < \xi_n$

$$\begin{aligned} K\psi_2(x, \tau) &= -\sum_{n=1}^N \frac{\lambda}{2\eta\delta} (e^{-\eta(-x+\xi_n)} [-4a_n^{(1)} + 2a_n^{(2)} + 2a_n^{(3)}] \\ &+ e^{\frac{\eta}{2}(-\delta+2x-2\xi_n)} [2a_n^{(1)} - 2a_n^{(2)} - \eta\delta a_n^{(2)}] \\ &+ e^{-\frac{\eta}{2}(\delta+2x-2\xi_n)} [2a_n^{(1)} - 2a_n^{(3)} - \eta\delta a_n^{(3)}] \\ &+ 4\eta[x - \xi_n][a_n^{(1)} - a_n^{(3)}] + 2\eta\delta a_n^{(1)}) \end{aligned} \quad (74)$$

- For $\xi_n < x < \xi_n + \frac{\delta}{2}$

$$\begin{aligned} K\psi_3(x, \tau) &= -\sum_{n=1}^N \frac{\lambda}{2\eta\delta} (e^{-\eta(x-\xi_n)} [-4a_n^{(1)} + 2a_n^{(2)} + 2a_n^{(3)}] \\ &+ e^{\frac{\eta}{2}(-\delta+2x-2\xi_n)} [2a_n^{(1)} - 2a_n^{(2)} - \eta\delta a_n^{(2)}] \\ &+ e^{-\frac{\eta}{2}(\delta+2x-2\xi_n)} [2a_n^{(1)} - 2a_n^{(3)} - \eta\delta a_n^{(3)}] \\ &+ 4\eta[x - \xi_n][-a_n^{(1)} + a_n^{(2)}] + 2\eta\delta a_n^{(1)}) \end{aligned} \quad (75)$$

- For $x > \xi_n + \frac{\delta}{2}$

$$\begin{aligned} K\psi_4(x, \tau) &= -\sum_{n=1}^N \frac{\lambda}{2\eta\delta} (e^{-\eta(x-\xi_n)} [-4a_n^{(1)} + 2a_n^{(2)} + 2a_n^{(3)}] \\ &+ e^{\frac{\eta}{2}(\delta-2x+2\xi_n)} [2a_n^{(1)} - 2a_n^{(2)} - \eta\delta a_n^{(2)}] \\ &+ e^{-\frac{\eta}{2}(\delta+2x-2\xi_n)} [2a_n^{(1)} - 2a_n^{(3)} - \eta\delta a_n^{(3)}]) \end{aligned} \quad (76)$$

Note the test function $\Xi(x, \xi_c, \delta)$ reduces in the area $(\xi_c - \frac{\delta}{2}, \xi_c + \frac{\delta}{2})$ to

$$\phi_0(x) = \begin{cases} 2 \frac{x - \xi_c + \frac{\delta}{2}}{\delta} & \text{if } \xi_c - \frac{\delta}{2} \leq x \leq \xi_c \\ -2 \frac{x - \xi_c - \frac{\delta}{2}}{\delta} & \text{if } \xi_c \leq x \leq \xi_c + \frac{\delta}{2} \end{cases} \quad (77)$$

Since taking the inner product of the convolution with the test function $\Xi(x, \xi_c, \delta)$ yields a large expression, which does not give extra insight in the material, we refrain from inserting it into this appendix. Instead, we provide all five different possible overlaps, which can occur due to the difference between the position of the center ξ_c of $\Xi(x, \xi_c, \delta)$ and the center of the convolution ξ_n . To conclude this appendix we give the five overlaps.

- Overlap 1: $\xi_c > \xi_n + \frac{\delta}{2}$

$$2 \int_{\xi_c - \frac{\delta}{2}}^{\xi_c} K\psi_4(x, \tau) \frac{x - \xi_c + \frac{\delta}{2}}{\delta} dx - 2 \int_{\xi_c}^{\xi_c + \frac{\delta}{2}} K\psi_4(x, \tau) \frac{x - \xi_c - \frac{\delta}{2}}{\delta} dx \quad (78)$$

- Overlap 2: $\xi_c = \xi_n + \frac{\delta}{2}$

$$2 \int_{\xi_c - \frac{\delta}{2}}^{\xi_c} K\psi_3(x, \tau) \frac{x - \xi_c + \frac{\delta}{2}}{\delta} dx - 2 \int_{\xi_c}^{\xi_c + \frac{\delta}{2}} K\psi_4(x, \tau) \frac{x - \xi_c - \frac{\delta}{2}}{\delta} dx \quad (79)$$

- Overlap 3: $\xi_c = \xi_n$

$$2 \int_{\xi_c - \frac{\delta}{2}}^{\xi_c} K\psi_2(x, \tau) \frac{x - \xi_c + \frac{\delta}{2}}{\delta} dx - 2 \int_{\xi_c}^{\xi_c + \frac{\delta}{2}} K\psi_3(x, \tau) \frac{x - \xi_c - \frac{\delta}{2}}{\delta} dx \quad (80)$$

- Overlap 4: $\xi_c = \xi_n - \frac{\delta}{2}$

$$2 \int_{\xi_c - \frac{\delta}{2}}^{\xi_c} K\psi_1(x, \tau) \frac{x - \xi_c + \frac{\delta}{2}}{\delta} dx - 2 \int_{\xi_c}^{\xi_c + \frac{\delta}{2}} K\psi_2(x, \tau) \frac{x - \xi_c - \frac{\delta}{2}}{\delta} dx \quad (81)$$

- Overlap 5: $\xi_c < \xi_n - \frac{\delta}{2}$

$$2 \int_{\xi_c - \frac{\delta}{2}}^{\xi_c} K\psi_1(x, \tau) \frac{x - \xi_c + \frac{\delta}{2}}{\delta} dx - 2 \int_{\xi_c}^{\xi_c + \frac{\delta}{2}} K\psi_1(x, \tau) \frac{x - \xi_c - \frac{\delta}{2}}{\delta} dx \quad (82)$$

References

- Ande00 Andersen, L. & Andreasen, J., Jump-diffusion processes: volatility smile fitting and numerical methods for option pricing. *Review of Derivatives Research*, 4 (2000), p. 231-261
- Barz99 Barz, G.L., Stochastic financial models for electricity derivatives. PhD dissertation, Stanford University (1999)
- Bert96 Bertoin, J., Lévy processes. Cambridge University Press, Cambridge (1996)
- Bjor97 Bjork, T., di Masi, G., Kabanov, Y. & Runngaldier, W., Towards a General Theory of Bond Markets. *Finance and Stochastics*, 1 (1997), p. 141-174
- Carr03 Carr, P., Geman, H., Madan, D., Yor, M., Stochastic Volatility for Levy Processes. Forthcoming in *Mathematical Finance* (2003).
- DelB00 Del Buono, M.A., The deregulation of electricity markets: promises made, challenges faced. PhD dissertation, Stanford University (2000)
- Deng99 Deng, S., Stochastic models of energy commodity prices and their applications: mean-reversion with jumps and spikes. Working paper, Georgia Institute of Technology (1999)
- Duff00 Duffie, D., Pan, J. & Singleton, K., Transform analysis and asset pricing for affine jump-diffusions. *Econometrica*, 68 (2000), p. 1343-1376
- Dupi94 Dupire, B., Pricing with a smile. *Risk*, 7 (1994) 1, p. 18-20
- EP97 European Parliament, Internal market for energy: common rules for the internal market in electricity.
<http://europa.eu.int/scadplus/leg/en/lvb/l27005.htm>
- EP01 European Parliament, Completing the internal energy market: revision of the electricity and gas directives.
<http://europa.eu.int/scadplus/leg/en/lvb/l27040.htm>
- Ethe02 Etheridge, A., A course in Financial Calculus. Oxford University Press, Oxford (2002)
- Glas03 Glasserman, P. & Kou, S.G., The term structure of simple forward rates with jump risk. Forthcoming in *Mathematical Finance* (2003)
- Hami90 Hamilton, J. D., Analysis of time series subject to changes in regime. *Journal of Econometrics*, 45 (1990), p. 39-70
- Hest93 Heston, S.L., A closed-form solution for options with stochastic volatility with applications to bond and currency options. *Review of Financial Studies*, 6 (1993) 2, p. 327-343

- Iked81 Ikeda, N. & Watanabe, S., Stochastic differential equations and diffusion processes. North Holland, Amsterdam and Kodansha, Tokyo (1981)
- Kall99 Kallsen, J. A utility maximization approach to hedging in incomplete markets. *Mathematical Methods of Operations Research*, 50 (1999), p. 321-338
- Khol01 Kholodnyi, V.A., A non-Markovian process for power prices with spikes and valuation of European contingent claims on power. Preprint, TXU-RAG-01/00 (2001)
- Kou01 Kou, S.G. & Wang, H., Option pricing under a double exponential jump diffusion model. Working paper, Columbia University (2001)
- Lewi01 Lewis, A.L., A simple option formula for general jump-diffusion and other exponential Levy processes (2001)
- Mert76 Merton, R.C., Option pricing when underlying stock returns are discontinuous. *Journal of Financial Economics*, 3 (1976) 1-2, p. 125-144
- Pete98 Peterson, A.F. Ray, S.L. & Mitra, R., Computational methods for electromagnetics (IEEE/OUP series on electromagnetic wave theory). Oxford University Press, Oxford (1998)
- Pilo98 Pilopovic, D., Energy risk: valuing and managing energy derivatives. McGraw-Hill Inc., New York (1998)
- Raib00 Raible, S., Lévy processes in finance: theory, numerics, and empirical facts, PhD dissertation, Albert-Ludwigs-Universität Freiburg (2000)
- Shiu99 Gerber, H.U. & Shiu, E.S., An actuarial bridge to option pricing. Chapter 6 in SOA Monograph M-AS99-2, (1999) p. 45-62
- Simo83 Simon, L. & Baderko, E.A., Linear PDE of second order. Tankönyvkiadó, Budapest (1983)
- Schw92 Schweizer, M., Mean-variance hedging for general claims. *The Annals of Applied Probability*, 2 (1992) 1, p. 171-179